

Molecular dynamics simulation of a confined Gay-Berne fluid

Guido Germano*, Michael P. Allen*, Denis Andrienko

H.H. Wills Physics Laboratory, Tyndall Avenue, Bristol BS8 1TL, England

*Currently visiting MPI für Polymerforschung and Institute of Physics, Mainz

1 Introduction

The phase diagram of soft rigid ellipsoidal particles interacting with the Gay-Berne (GB) potential [1] has been studied thoroughly some time ago [2] (Fig. 1). The GB potential is similar to the Lennard-Jones potential, but has well depth (ε) and range (σ) parameters dependent on molecular orientations:

$$\begin{aligned}
 U_{ij}(\mathbf{r}_{ij}, \mathbf{e}_i, \mathbf{e}_j) &= 4\varepsilon(\hat{\mathbf{r}}_{ij}, \mathbf{e}_i, \mathbf{e}_j) \left[\varrho_{ij}^{12}(\mathbf{r}_{ij}, \mathbf{e}_i, \mathbf{e}_j) - \varrho_{ij}^6(\mathbf{r}_{ij}, \mathbf{e}_i, \mathbf{e}_j) \right] \\
 \text{where } \varrho_{ij}(\mathbf{r}_{ij}, \mathbf{e}_i, \mathbf{e}_j) &= \frac{\sigma_0}{r_{ij} - \sigma(\hat{\mathbf{r}}_{ij}, \mathbf{e}_i, \mathbf{e}_j) + \sigma_0} \\
 \sigma(\hat{\mathbf{r}}_{ij}, \mathbf{e}_i, \mathbf{e}_j) &= \sigma_0 \left\{ 1 - \frac{\chi}{2} \left[\frac{(\hat{\mathbf{r}}_{ij} \cdot \mathbf{e}_i + \hat{\mathbf{r}}_{ij} \cdot \mathbf{e}_j)^2}{1 + \chi(\mathbf{e}_i \cdot \mathbf{e}_j)} + \frac{(\hat{\mathbf{r}}_{ij} \cdot \mathbf{e}_i - \hat{\mathbf{r}}_{ij} \cdot \mathbf{e}_j)^2}{1 - \chi(\mathbf{e}_i \cdot \mathbf{e}_j)} \right] \right\}^{-1/2} \\
 \varepsilon(\hat{\mathbf{r}}_{ij}, \mathbf{e}_i, \mathbf{e}_j) &= \varepsilon_0 [\varepsilon_1(\mathbf{e}_i, \mathbf{e}_j)]^\nu [\varepsilon_2(\hat{\mathbf{r}}_{ij}, \mathbf{e}_i, \mathbf{e}_j)]^\mu \\
 \varepsilon_1(\mathbf{e}_i, \mathbf{e}_j) &= [1 - \chi^2(\mathbf{e}_i \cdot \mathbf{e}_j)^2]^{-1/2} \\
 \varepsilon_2(\hat{\mathbf{r}}_{ij}, \mathbf{e}_i, \mathbf{e}_j) &= 1 - \frac{\chi'}{2} \left[\frac{(\hat{\mathbf{r}}_{ij} \cdot \mathbf{e}_i + \hat{\mathbf{r}}_{ij} \cdot \mathbf{e}_j)^2}{1 + \chi'(\mathbf{e}_i \cdot \mathbf{e}_j)} + \frac{(\hat{\mathbf{r}}_{ij} \cdot \mathbf{e}_i - \hat{\mathbf{r}}_{ij} \cdot \mathbf{e}_j)^2}{1 - \chi'(\mathbf{e}_i \cdot \mathbf{e}_j)} \right].
 \end{aligned}$$

$\chi = (\kappa^2 - 1)/(\kappa^2 + 1)$ where κ is the ratio of the molecular length to the molecular diameter σ_0 ; $\chi' = (\kappa'^{1/\mu} - 1)/(\kappa'^{1/\mu} + 1)$ where κ' is the ratio between the minimum of the potential for a pair of parallel side-by-side molecules and the minimum of the potential for a pair of parallel end-to-end molecules; ε_0 is a parameter that sets the overall energy scale of the pair interactions.

The pair potential is truncated at a distance $r_{\text{cut}} = (\kappa + 1)\sigma_0$ and shifted such that $U(r_{ij} = r_{\text{cut}}) = 0$:

$$U(\mathbf{r}_{ij}, \mathbf{e}_i, \mathbf{e}_j) = U^{\text{GB}}(r_{ij}\hat{\mathbf{r}}_{ij}, \mathbf{e}_i, \mathbf{e}_j) - U^{\text{GB}}(r_{\text{cut}}\hat{\mathbf{r}}_{ij}, \mathbf{e}_i, \mathbf{e}_j).$$

More recently [3] the GB fluid has been investigated in slab geometry, with no periodic boundary conditions along the z direction and two parallel confining surfaces that extend infinitely along the x and y directions; the surface interaction depends only on two variables, z and e_z , and favors a 40° tilted orientation of the particles close to the surface (Figs. 1, 1, 1).

$$\begin{aligned}
 U_i^s(z_i, e_{z,i}) &= \alpha \varepsilon^s(e_{z,i}) \left[\frac{2}{15} \varrho_i^{s9}(z_i, e_{z,i}) - \varrho_i^{s3}(z_i, e_{z,i}) \right] \\
 \text{where } \varrho_i^s(z_i, e_{z,i}) &= \frac{\sigma_0}{z_i - \sigma^s(e_{z,i}) + \sigma_0} \\
 \sigma^s(e_{z,i}) &= \sigma_0 (1 - \chi e_{z,i}^2)^{-1/2} \\
 \varepsilon^s(e_{z,i}) &= \varepsilon_0 (1 - \chi' e_{z,i}^2)^\mu.
 \end{aligned}$$

α is a parameter that governs the relative strength of the surface and the pair potentials, and z is the distance from one of the two surfaces. Every particle always interacts with both surfaces: U^s is not truncated.

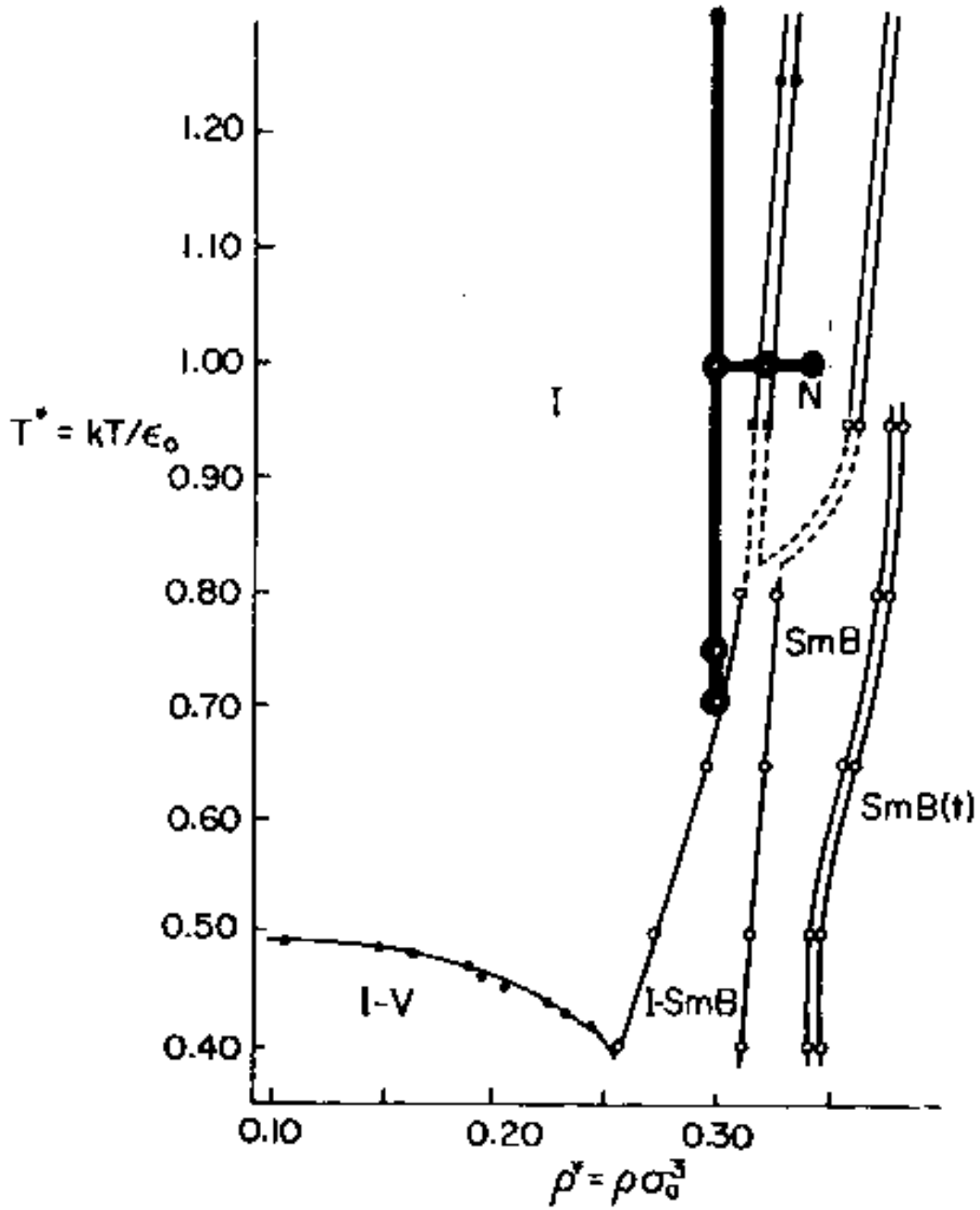


Figure 1: Bulk phase diagram of the Gay-Berne fluid with $\kappa = 3, \kappa' = 5, \mu = 2, \nu = 1$ (from Fig. 16 of Ref. [2]). The two thick vertical and horizontal lines connect the state points studied in this work. A further point at $\rho = 0.3, T = 1.5$ is out of scale.

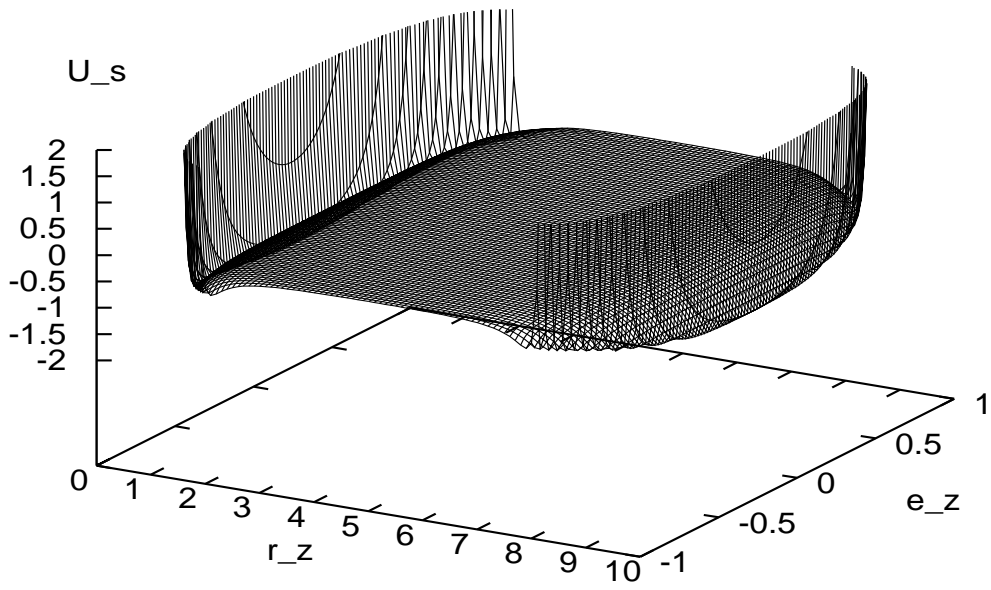


Figure 2: Potential energy of a particle due to interaction with the surfaces.

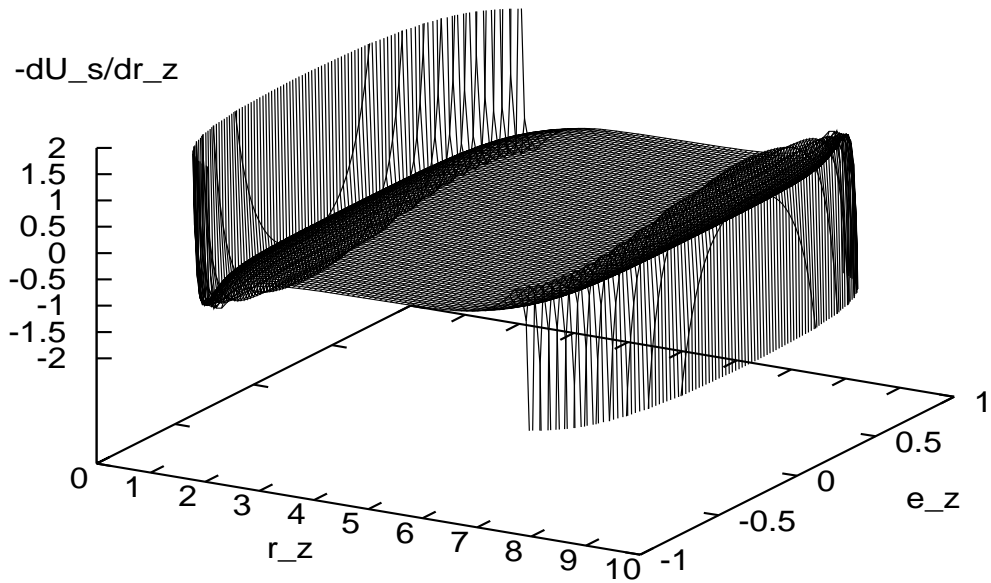


Figure 3: Force exerted on a particle by the surfaces.

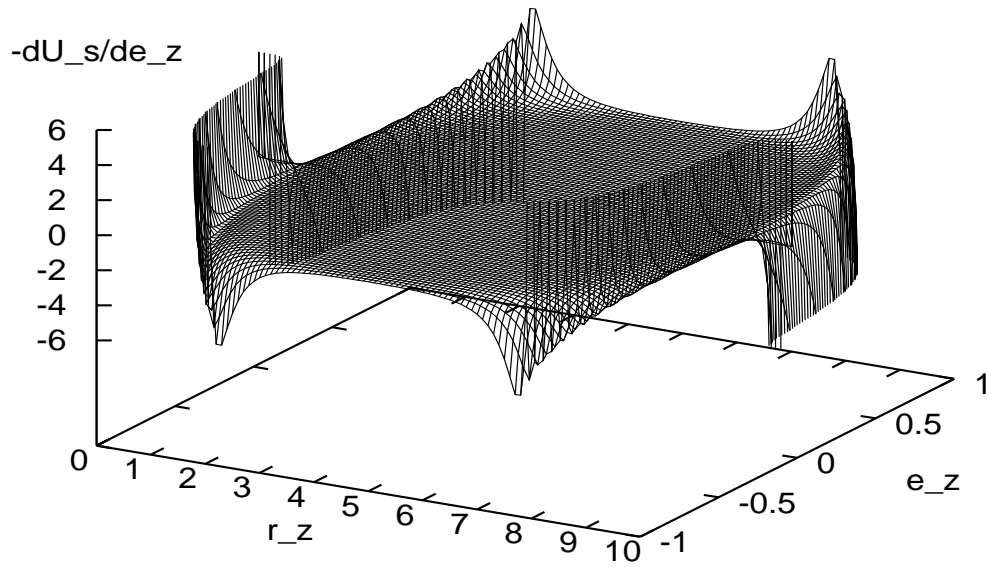


Figure 4: Gorque exerted on a particle by the surfaces.

In Ref. [3] a system of 256 particles was examined on an isochore line with $\rho \cong 0.3$. At the end of a cooling run from $T = 1.5$ to $T = 0.7$ with $\alpha = 1.0$ the time-averaged density $\overline{\rho(z)}$ is reported to develop “regular, large amplitude modulations which traverse the whole of the slab” (Figs. 1, 1).

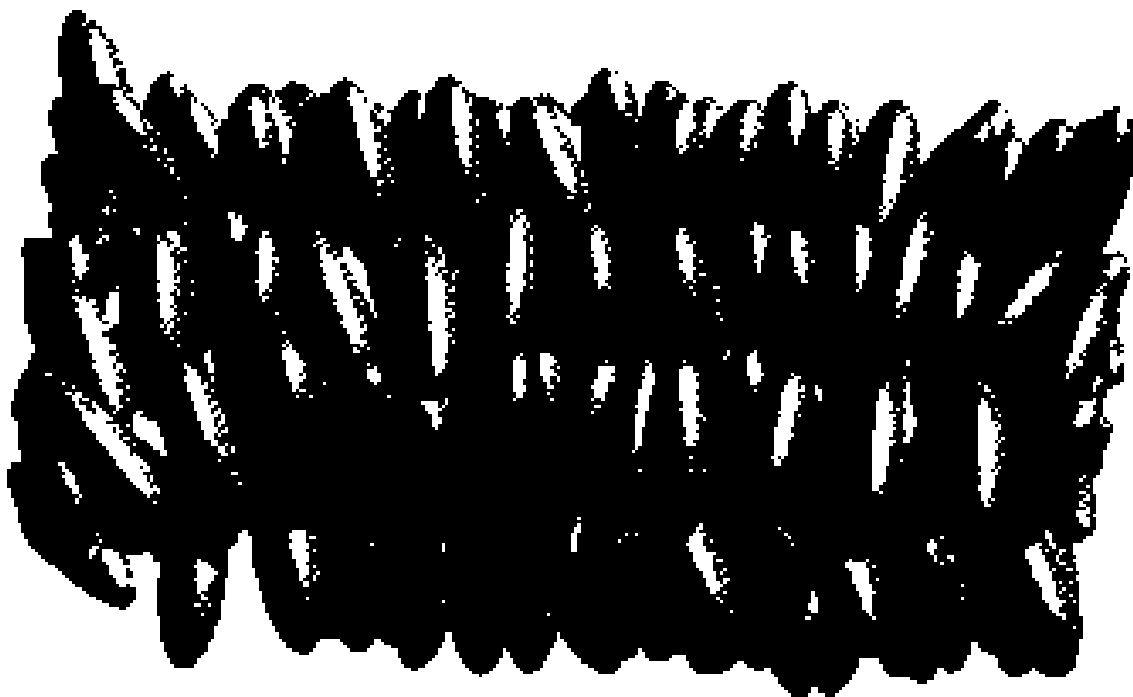


Figure 5: System snapshot at $\rho = 0.3, T = 0.7$ (from fig. 8d of Ref. [3]).

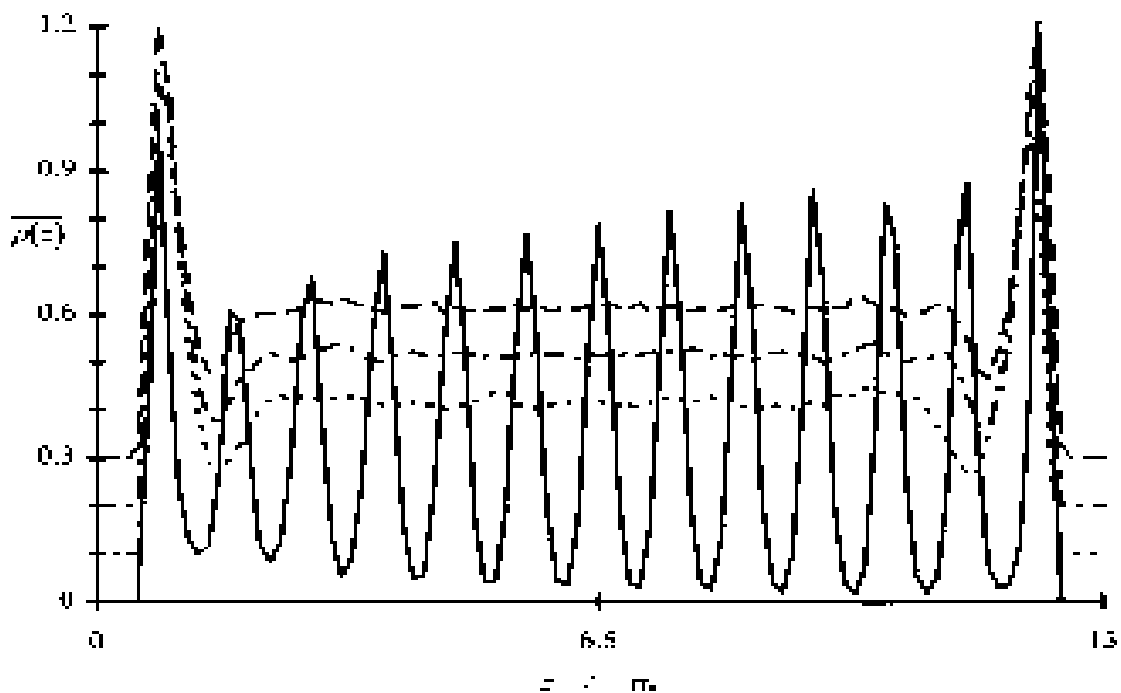


Figure 6: Time-averaged density profiles at $\rho = 0.3$ (from Fig. 2 of Ref. [3]). $T = 0.7$ (solid line); $T = 0.75$ (dotted line); $T = 1.0$ (dash-dotted line); $T = 1.5$ (dashed line). Successive curves have been shifted by 0.1 along the ρ axis to aid resolution.

2 Results

As a preliminary study we reproduced the results of Ref. [3], except for the modulations of $\rho(z)$ at $T = 0.7$ that we could not observe (Fig. 2).

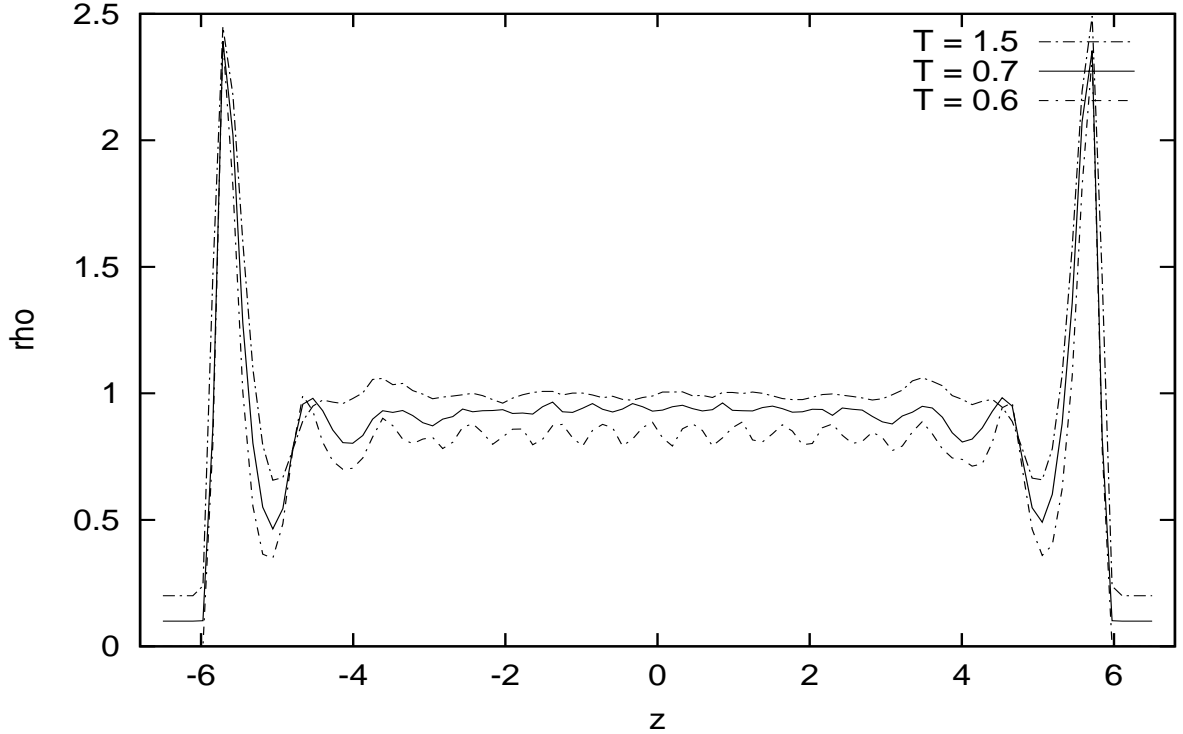


Figure 7: Time-averaged density profiles at $\rho = 0.3$. Successive curves have been shifted by 0.1 along the ρ axis to aid resolution.

Then we replicated the starting body-centered cubic lattice 10 times along z and 2 times each along x and y , obtaining a bigger and more elongated box with 10240 particles (Fig. 2). Indeed a system size of 256 is appropriate to study a bulk phase with periodic boundary conditions in all directions, but seems too small for a slab geometry, because the surfaces are too close to each other.

We melted the lattice at $T = 1.5$ and equilibrated it at $\rho \cong 0.3$. As in Ref. [3], we cooled it down in three steps at $T = 1.0$, $T = 0.75$ and $T = 0.7$ (Figs. 2, 2, 2, 2). Again we did not observe any modulations of $\rho(z)$ at $T = 0.7$; instead, a highly ordered phase started forming in the middle of the box, so our first conclusion was that the density modulations reported in Ref. [3] are not peculiar of the slab geometry, but are simply a feature of a highly ordered smectic phase: the state point $\rho \cong 0.3, T = 0.7$ is very close to the isotropic/smectic B coexistence region in the bulk phase diagram of this system (Fig. 1).

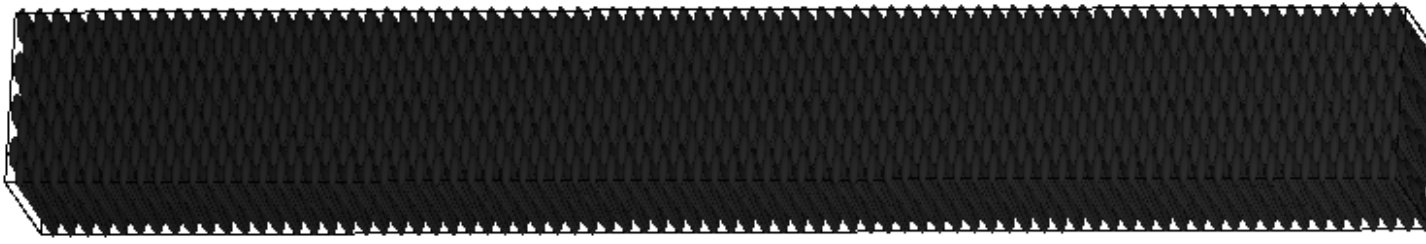


Figure 8: System snapshot at start.

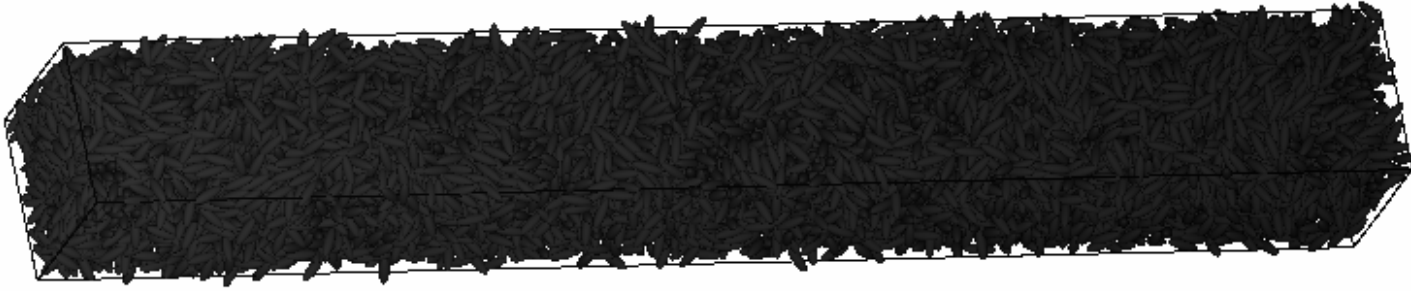


Figure 9: System snapshot at $\rho = 0.3, T = 1.0$.



Figure 10: System snapshot at $\rho = 0.3, T = 0.7$.

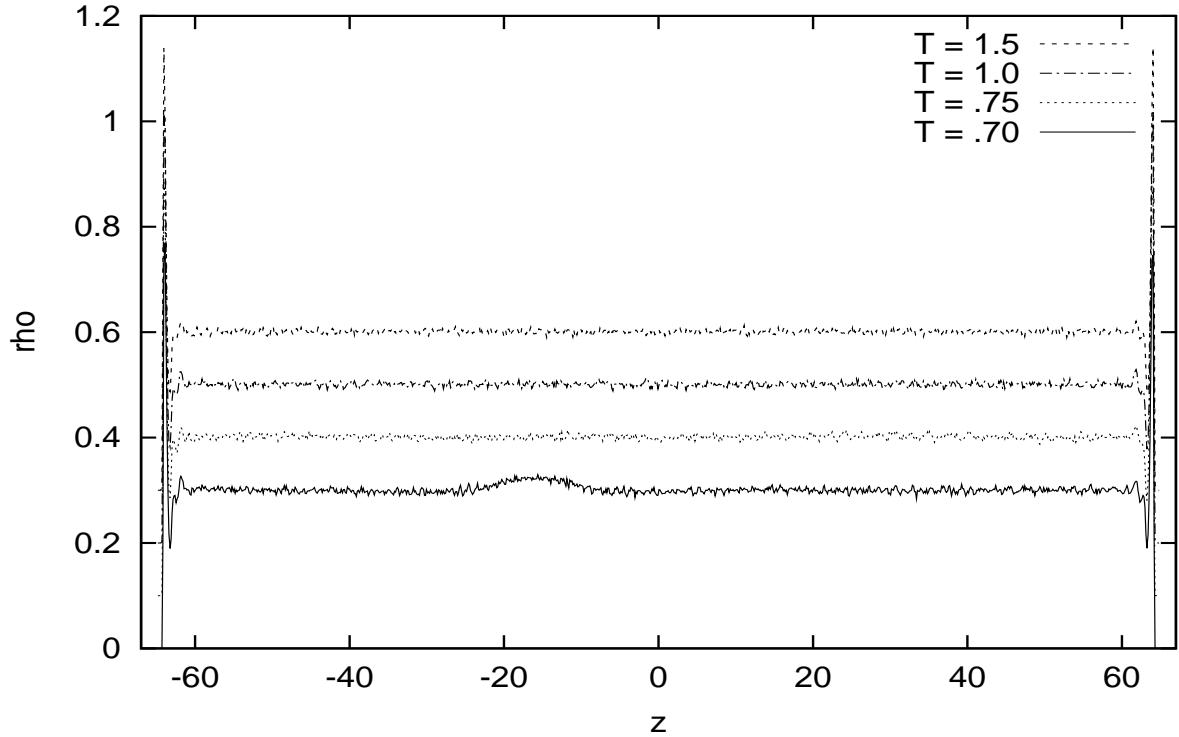


Figure 11: Time-averaged density profiles at $\rho = 0.3$. Successive curves have been shifted by 0.1 along the ρ axis to aid resolution.

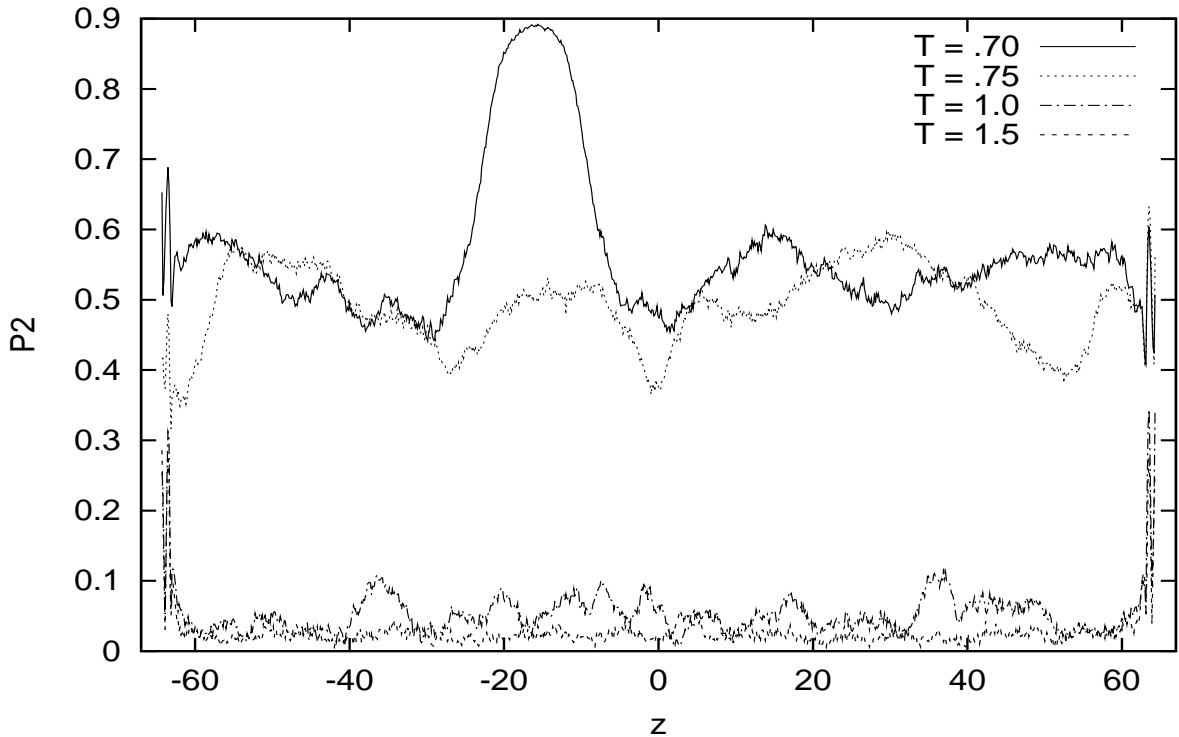


Figure 12: Time-averaged order parameter profiles at $\rho = 0.3$.

Due to long equilibration times in the coexistence region, we did not pursue this point further, and instead ventured into the nematic phase along an isotherm starting from $\rho \cong 0.3, T = 1.0$. So far we examined two state points with $\rho \cong 0.32$ and $\rho \cong 0.34$ (Figs. 2, 2, 2).



Figure 13: System snapshot at $\rho = 0.34, T = 1.0$.

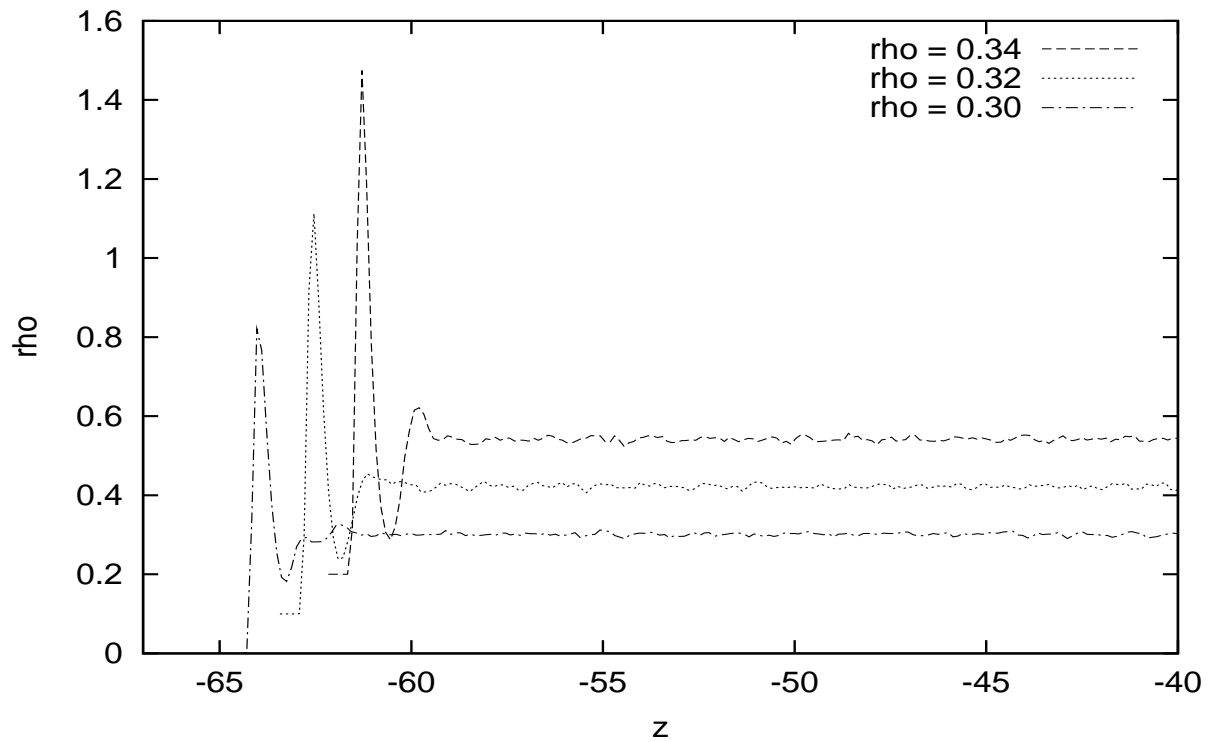


Figure 14: Time-averaged density profiles at $T = 1.0$ close to the left surface. Successive curves have been shifted by 0.1 along the ρ axis to aid resolution.

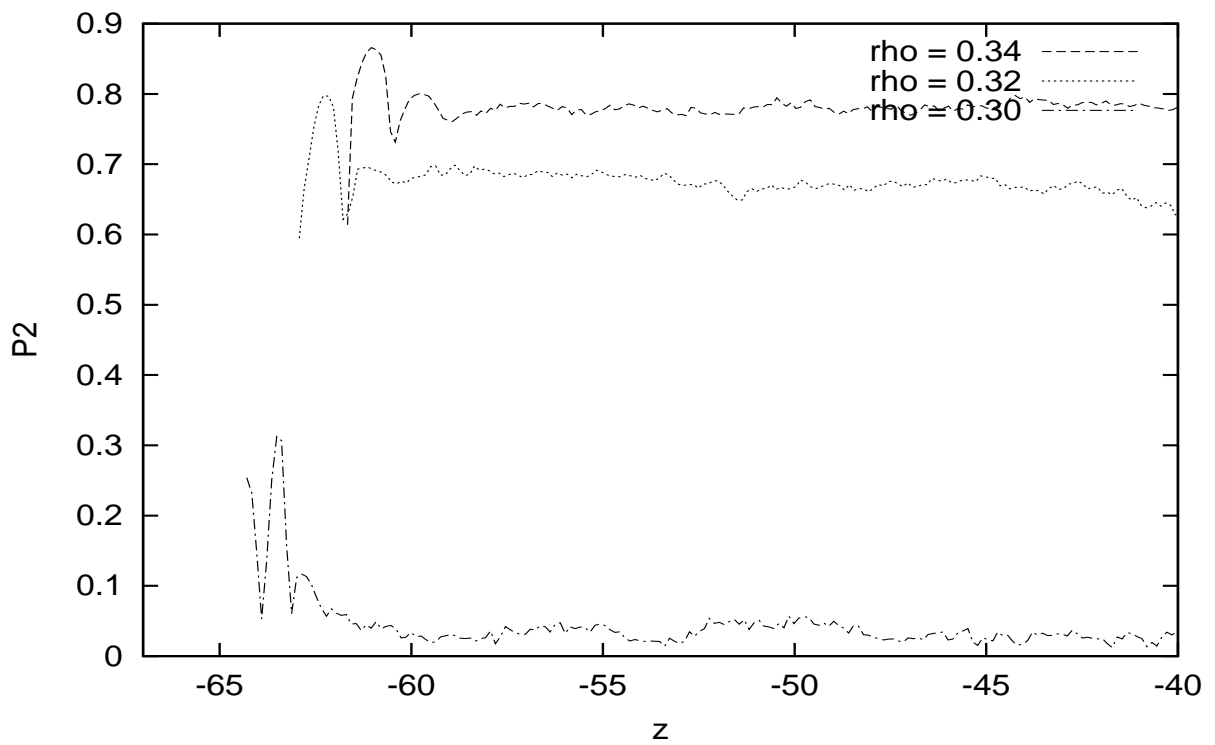


Figure 15: Time-averaged order parameter profiles at $T = 1.0$ close to the left surface.

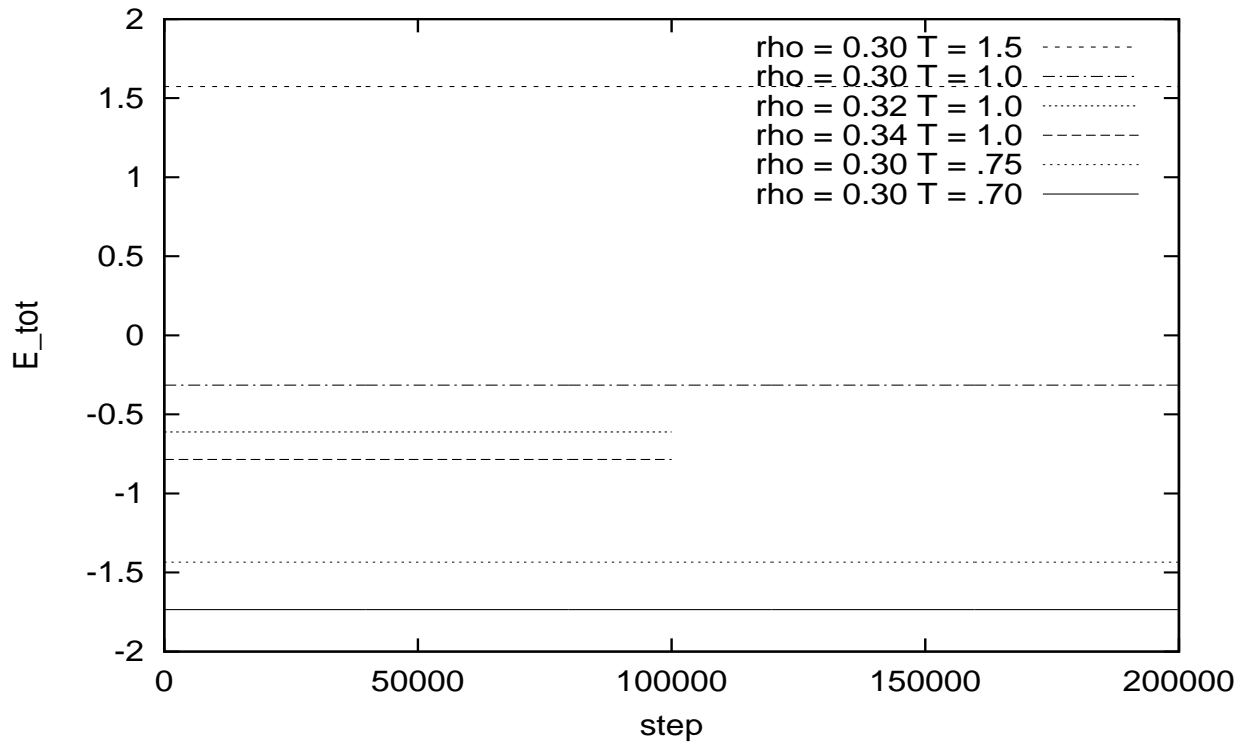


Figure 16: The total energy is conserved perfectly in the microcanonical ensemble, with absolutely no drift and $\Delta E/E$ values ranging between $2E-6$ and $2E-5$. We used a version of the velocity Verlet algorithm for uniaxial particles.

3 Conclusions and outlook

Unlike stated in Ref. [3], this potential does not show any long range effects away from the surfaces, so we will concentrate on studying the behavior of the fluid close to one of them. Nevertheless, the simulation box must be big enough to clearly rule out any influence on one surface layer by the opposite surface (the presence of two surfaces is unavoidable in this kind of simulation).

4 Computational details

We ran the 256-particle system on a personal computer with a standard scalar molecular dynamics (MD) program. As usual, we employed a spherical cutoff for the pair interactions; strangely, this was not done in Ref. [3]. We resorted to a Cray T3E for the 10240-particle system and used GBMEGA, our own domain decomposition parallel MD program for rigid bodies with axial symmetry. Along the isochore we allowed 500 000 steps for equilibration at each state point and sampled in the microcanonical ensemble for another 200 000 steps, as in Ref. [3]. Along the isotherm we deemed 200 000 equilibration steps and 100 000 production steps per point enough. The computational cost on the T3E was about 8 processor hours per 10 000 steps with good speedups in the 8-64 nodes range.

Acknowledgements

Discussions with the group of Doug Cleaver and other members of the High Performance Computing consortium for Statistical Mechanics of Complex Fluids are gratefully acknowledged. This work was supported by the Engineering and Physical Sciences Research Council. GG's stay in Mainz was made possible by a British Council grant and MPA's by a fellowship of the Alexander von Humboldt-Stiftung.

References

- [1] J. G. Gay and B. J. Berne, *J. Chem. Phys.* **74**, 3316 (1981).
- [2] E. De Miguel, L. F. Rull, M. K. Challam, M. K. E. Gubbins, *Mol. Phys.* **74**, 405-424 (1991).
- [3] G. D. Wall, D. J. Cleaver, *Phys. Rev. E* **56**, 4306-4316 (1997)